

CrossMark
click for updates

Cite this: DOI: 10.1039/c5tc01065a

Effect of the molecular structure of the host materials on the lifetime of green thermally activated delayed fluorescent organic light-emitting diodes†

Yirang Im, Wook Song and Jun Yeob Lee*

Two dibenzothiophene derived compounds, 4-(3-(triphenylen-2-yl)phenyl)dibenzo[*b,d*]thiophene (DBTTP1) and 4-(5'-phenyl-[1,1':3',1''-terphenyl]-3-yl)dibenzo[*b,d*]thiophene (DBTTP2), were prepared as the host materials for green thermally activated delayed fluorescent (TADF) emitters to investigate the effect of the molecular structure of the host materials on the efficiency and lifetime of the green TADF devices. The green TADF devices fabricated using the DBTTP1 host material exhibited a high quantum efficiency of above 20% and a lifetime longer than 250 h up to 80% of initial luminance at 1000 cd m⁻². Comparing the two host materials, triphenylene modified DBTTP1 was better than terphenyl modified DBTTP2 in terms of the lifetime of the green TADF devices.

Received 16th April 2015,
Accepted 30th June 2015

DOI: 10.1039/c5tc01065a

www.rsc.org/MaterialsC

Introduction

Thermally activated delayed fluorescent (TADF) devices have been actively researched for the last couple of years because of the potential high quantum efficiency of TADF emitters achieved *via* the reverse intersystem crossing process.^{1–8} Simultaneous singlet and triplet exciton harvesting by the reverse intersystem crossing process already demonstrated a high quantum efficiency close to 20% in the green and blue TADF organic light-emitting diodes (OLEDs).^{4–8}

The significant enhancement in the quantum efficiency of the TADF devices was mostly achieved by the development of the host and TADF emitters. The TADF emitters determined the maximum quantum efficiency achievable by engineering the device structure and the host materials played a role of realizing the maximum quantum efficiency of the TADF emitters. For example, the quantum efficiency of a well-known TADF emitter, (4*s*,6*s*)-2,4,5,6-tetra(9*H*-carbazol-9-yl)isophthalonitrile (4CzIPN), was reported to be 19.3% in the first work by Adachi *et al.*,⁸ but it was increased to above 20% by optimizing the hosts of the 4CzIPN emitting layer.^{9–11}

As described above, the quantum efficiency of the TADF devices already reached the same level as that of phosphorescent OLEDs, but the lifetime of the TADF OLEDs was not widely studied. There were only a few papers reporting on the lifetime

of the TADF devices,^{7,9,12} and it was demonstrated that the lifetime of the 4CzIPN TADF device is as long as that of phosphorescent OLEDs under the same driving conditions.¹³ Host materials such as 3,3-di(9*H*-carbazol-9-yl)biphenyl¹² and 3',5'-di(carbazol-9-yl)-[1,1'-biphenyl]-3,5-dicarbonitrile⁹ were efficient in extending the lifetime of the TADF OLEDs. However, no systematic study was carried out to study the relationship between the molecular structure of the host materials and the lifetime of the TADF OLEDs. Therefore, further study to improve the lifetime of the TADF devices by engineering the chemical structure of the host materials is required.

Herein, we explain the effect of the chemical structure of the host materials on the lifetime of green TADF OLEDs using dibenzothiophene derived host materials. Two dibenzothiophene based materials, 4-(3-(triphenylen-2-yl)phenyl)dibenzo[*b,d*]thiophene (DBTTP1) and 4-(5'-phenyl-[1,1':3',1''-terphenyl]-3-yl)dibenzo[*b,d*]thiophene (DBTTP2), were chosen as the host materials for 4CzIPN and the lifetime of the TADF OLEDs was investigated. It was proven that the DBTTP1 host with a triphenylene moiety is better than the DBTTP2 host with a terphenyl moiety.

Experimental section

General information

3-Bromiodobenzene (TCI Chem. Co.) was used without further purification. 1,3,5-Tribromobenzene, *n*-butyl lithium, triethyl borate (Aldrich Chem. Co.), potassium carbonate (K₂CO₃), hydrochloric acid (HCl) (Duksan Sci. Co.), dibenzothiophene-4-boronic acid (Alfa Aesar Co.), phenyl boronic acid, and

School of Chemical and Engineering, Sunkyoungwan University, 2066, Seobu-ro, Jangan-gu, Suwon-si, Gyeonggi-do, 448-701, Korea. E-mail: leej17@skku.edu;

Fax: +82-31-299-4716; Tel: +82-31-299-4716

† Electronic supplementary information (ESI) available. See DOI: 10.1039/c5tc01065a

tetrakis(triphenylphosphine) palladium(0) ($\text{Pd}(\text{PPh}_3)_4$) (P&H tech Co.) were also used as received. The general analysis method for the synthesized compounds is described in a previous study.⁹

Synthesis

DBTTP1 was synthesized according to the method reported in the literature¹⁴ and the synthetic scheme of DBTTP2 is represented in Scheme 1.

5'-Bromo-1,1':3',1''-terphenyl (1). 5'-Bromo-1,1':3',1''-terphenyl was synthesized according to the literature method.¹⁵

[1,1':3',1''-Terphenyl]-5'-ylboronic acid (2). Compound 1 (5 g, 16.17 mmol) was added to dry tetrahydrofuran (60 ml) and the solution was stirred at -78°C . Then, 2.5 M *n*-BuLi (7.7 ml) was added and triethyl borate (3.30 ml, 19.40 mmol) was added to the reaction mixture after 2 h. The resulting solution was stirred for 24 h under a nitrogen atmosphere and then the mixture was quenched with 2 M HCl solution. The solution was extracted with ethyl acetate and distilled water (DW). The organic layer was dried over anhydrous MgSO_4 and evaporated *in vacuo* to give a crude product. The synthesized [1,1':3',1''-terphenyl]-5'-ylboronic acid was used in the next reaction without further purification. A white powder was obtained as a product (4.3 g, yield: 97%).

4-(3-Bromophenyl)dibenzo[*b,d*]thiophene (3). 4-(3-Bromophenyl)dibenzo[*b,d*]thiophene was synthesized according to the method described in the literature.¹⁶

4-(5'-Phenyl-[1,1':3',1''-terphenyl]-3-yl)dibenzo[*b,d*]thiophene (DBTTP2). Compound 2 (0.2 g, 0.59 mmol), compound 3 (0.19 g, 0.71 mmol), and K_2CO_3 (0.24 g, 1.70 mmol) were dissolved in tetrahydrofuran (100 ml) and DW (20 ml) by bubbling with nitrogen for 30 min. $\text{Pd}(\text{PPh}_3)_4$ (0.2 g, 0.18 mmol) was added to the solution and the resulting solution was refluxed for 24 h under a nitrogen atmosphere. The mixture was diluted with ethyl acetate and washed with DW. The organic layer was dried over anhydrous MgSO_4 and evaporated *in vacuo* to give a crude product. The extract was evaporated to dryness, affording a white solid, which was further purified by column chromatography

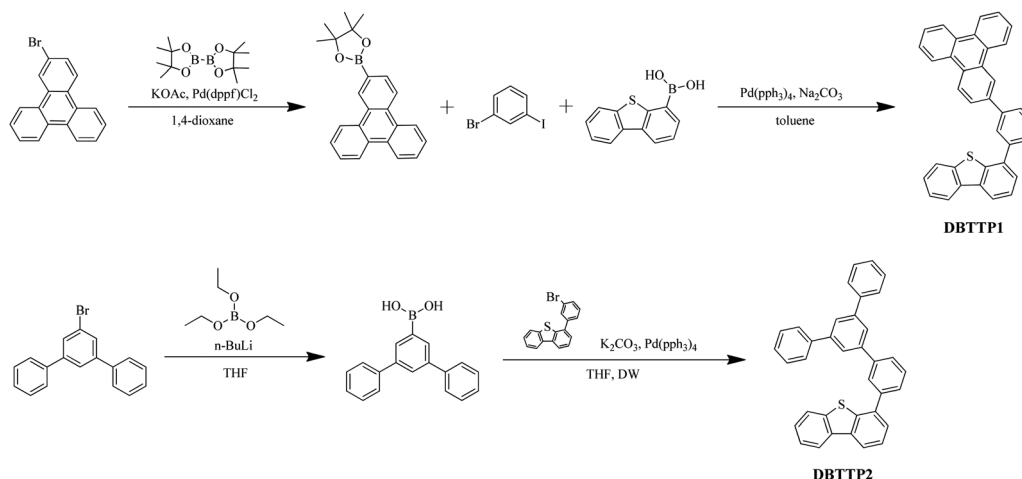
using methylene chloride/hexane as an eluent. A white powder was obtained after vacuum train sublimation.

Yield 32%, ^1H NMR (400 MHz, CDCl_3): δ 8.19–8.13 (m, 2H), 8.08 (t, 1H, $J = 1.60$ Hz), 7.87 (d, 2H, $J = 2.00$ Hz), 7.84–7.79 (m, 2H), 7.75–7.74 (m, 2H), 7.72–7.69 (m, 4H), 7.61 (d, 1H, $J = 7.80$ Hz), 7.58–7.54 (m, 2H), 7.48–7.43 (m, 6H), 7.37 (t, 2H) ^{13}C NMR (400 MHz, CDCl_3): δ 142.65, 142.23, 141.91, 141.43, 141.29, 139.76, 138.86, 137.03, 136.51, 136.00, 129.58, 129.07, 127.78, 127.58, 127.52, 127.16, 127.04, 125.60, 125.45, 125.37, 124.62, 122.84, 121.96, 120.83 MS (FAB) m/z 489 $[(\text{M} + \text{H})^+]$. Elemental analysis (calculated for $\text{C}_{36}\text{H}_{24}\text{S}$): C, 88.49; H, 4.95; S, 6.56%. Found: C, 88.33; H, 4.91; S, 6.60%.

Device fabrication and measurements. Devices fabricated in this work were grown on an indium tin oxide (ITO, 120 nm) substrate cleaned using deionized water and 2-propanol. After drying and ultraviolet-ozone treatment for 10 min, poly-(3,4-ethylenedioxythiophene):poly(styrenesulfonate) (PEDOT:PSS, 60 nm) was spin-coated followed by vacuum evaporation of 4,4'-cyclohexylidenebis[*N,N*-bis(4-methylphenyl)aniline] (TAPC, 20 nm), 1,3-bis(*N*-carbazolyl)benzene (mCP, 10 nm), host:4CzIPN (25 nm), diphenylphosphine oxide-4-(triphenylsilyl)phenyl (TSPO1, 5 nm), 2,2,2''-(1,3,5-benzinetriyl)-tris(1-phenyl-1-*H*-benzimidazole) (TPBi) (30 nm), LiF(1 nm), and Al(200 nm). 4CzIPN was doped at doping concentrations of 3, 10, and 15%. Current density, voltage, and luminance data were collected by sweeping the voltage of the device. Electrical and optical performances were gathered using a Keithley 2400 source measurement unit and a CS 1000 spectroradiometer. Lifetime measurement of the device was performed at an initial luminance of 1000 cd m^{-2} in a constant current mode using a lifetime test system equipped with a photodiode to monitor the luminance change during the lifetime test.

Results and discussion

It is important to apply high triplet energy and chemically stable host materials for stable operation of the TADF OLEDs. At least, the triplet energy of the TADF host material should be



Scheme 1 Synthetic scheme of DBTTP2 and chemical structure of DBTTP1.

higher than that of the TADF dopant and the TADF host material should possess only stable chemical moieties in the backbone structure. Among several backbone structures, dibenzothiophene was chosen due to its planar aromatic structure which stabilizes the molecular structure, and it was substituted with aromatic moieties of triphenylene and terphenyl to compare the two moieties in terms of the lifetime of the devices.

DBTTP1 was synthesized according to the method reported in the literature¹⁴ and DBTTP2 was synthesized by Suzuki coupling reaction between a dibenzothiophene derived aromatic unit and boronic acid of terphenyl as described in Scheme 1. DBTTP2 was obtained in a synthetic yield of 32%. Vacuum train sublimation after purification by column chromatography provided DBTTP2 with a high purity level of above 99%. Chemical structure confirmation was carried out using a ¹H and ¹³C nuclear magnetic resonance spectrometer, a mass spectrometer and an elemental analyzer. The chemical structure of DBTTP1 is also added in Scheme 1.

The highest occupied molecular orbital (HOMO) and the lowest unoccupied molecular orbital (LUMO) of DBTTP1 and DBTTP2 are compared in Fig. 1. The HOMO of DBTTP1 was located on the dibenzothiophene unit, while the LUMO was localized on the triphenylene unit. In the case of DBTTP2, both the HOMO and LUMO were dispersed over dibenzothiophene. It tells us that the hole and electron transport properties of DBTTP1 would be dominated by the dibenzothiophene unit and the triphenylene unit, respectively, whereas those of DBTTP2 would be dictated by the dibenzothiophene unit. The LUMO localization on the triphenylene unit of DBTTP1 is due to its electron accepting character originating as a result of the aromatic nature of triphenylene.

UV-vis (ultraviolet-visible), solution photoluminescence (PL) and low temperature PL spectra of DBTTP2 are shown in Fig. 2. A strong π - π^* transition of the backbone structure of DBTTP2 was observed in the UV-vis absorption spectrum and an emission peak at 357 nm was detected in the solution PL spectrum. The UV-vis absorption edge was 344 nm, which was converted to a UV-vis gap of 3.61 eV. The peak position of phosphorescent emission was 457 nm, which corresponded to a triplet energy of

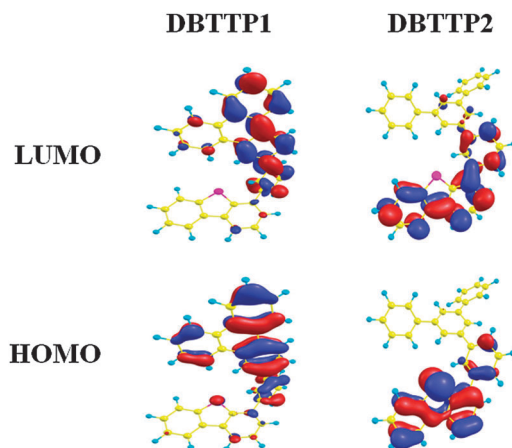


Fig. 1 HOMO and LUMO distribution of DBTTP1 and DBTTP2.

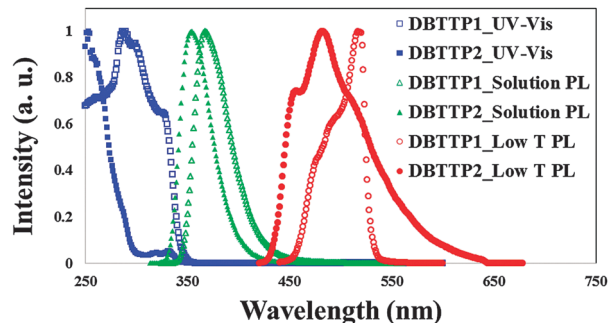


Fig. 2 UV-vis, solution PL and low temperature PL spectra of DBTTP1 and DBTTP2.

2.71 eV. The triplet energy of DBTTP2 was higher than that of DBTTP1 (2.64 eV) by 0.07 eV. The relatively low triplet energy of DBTTP1 is due to the low triplet energy of the triphenylene unit which has three benzene rings in the same plane. The three benzene rings of DBTTP2 distorted each other and raised the triplet energy of DBTTP2.

An electrochemical oxidation method namely cyclic voltammetry was used to measure the HOMO of DBTTP2. The oxidation curve of DBTTP2 is presented in Fig. 3. The oxidation onset of DBTTP2 was observed at 1.53 V and the HOMO level estimated from the oxidation onset was -6.33 eV in DBTTP2. The LUMO estimated from the HOMO and UV-vis gap was -2.72 eV. The electrochemical stability of DBTTP1 and DBTTP2 was also studied and the two materials showed fairly stable oxidation and reduction curves during multicycle CV scans as presented in the ESI.†

DBTTP1 and DBTTP2 were evaluated as the host materials of a common 4CzIPN TADF dopant because they have triplet energy higher than the singlet and triplet energy of 4CzIPN. Before device fabrication, the TADF behavior of 4CzIPN doped films was confirmed by transient PL measurement data in Fig. 4. It could be proven that the two host materials induce delayed emission of 4CzIPN. Fig. 5 represents the current density–voltage–luminance relationship of the DBTTP1 and DBTTP2 devices doped with 4CzIPN at a doping concentration of 3%. The current density and luminance were relatively high for the DBTTP1 device compared with the DBTTP2 device. The turn-on voltage of the device was 4.0 V and the driving voltages at 1000 cd m^{-2} were 5.7 V and 6.0 V for the DBTTP1 and

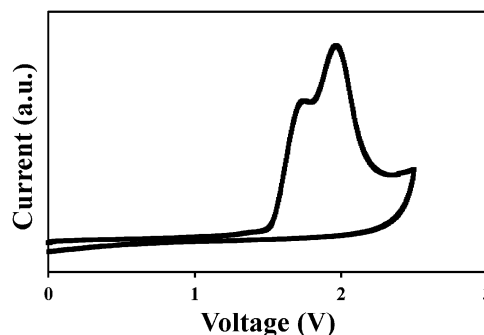


Fig. 3 Oxidation curve of DBTTP2.

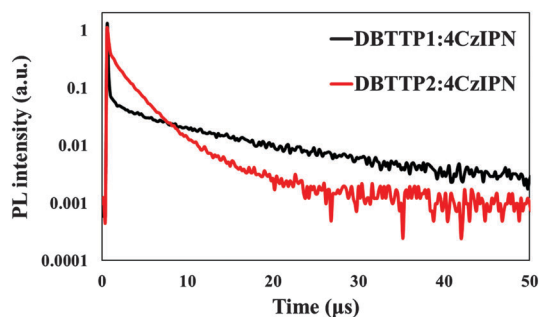


Fig. 4 Transient PL decay curves of DBTTP1:4CzIPN and DBTTP2:4CzIPN films.

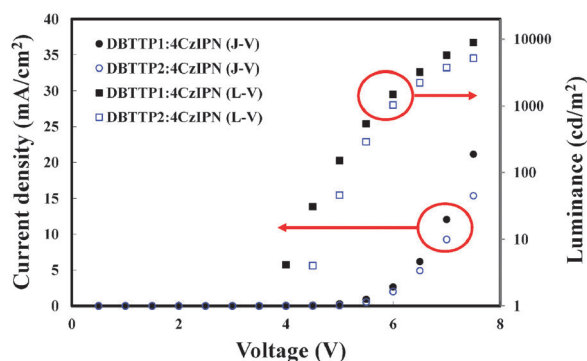


Fig. 5 Current density–voltage–luminance curves of the DBTTP1 and DBTTP2 devices doped with 4CzIPN at a doping concentration of 3%.

DBTTP2 devices, respectively. The relatively low driving voltage of DBTTP1 is due to the triphenylene moiety which is known as an electron transport moiety. Compared with a terphenyl moiety, the triphenylene moiety can increase the electron density in the emitting layer, which contributed to the high current density of the DBTTP1 device.

The quantum efficiency data of the DBTTP1 and DBTTP2 devices are represented according to the luminance of the device in Fig. 6. The quantum efficiency was relatively high for the DBTTP2 device, and was 20.0% at 46 cd m^{-2} and 17.5% at 1000 cd m^{-2} . Although the maximum quantum efficiency of

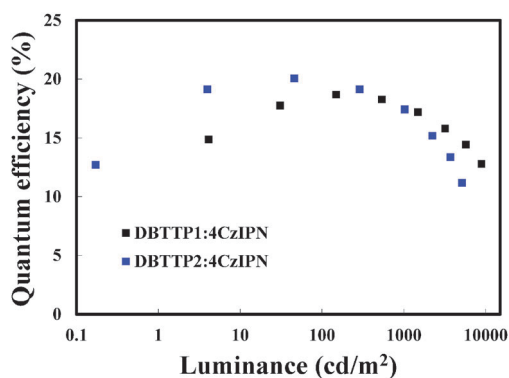


Fig. 6 Quantum efficiency–luminance plots of the DBTTP1 and DBTTP2 devices.

the DBTTP1 device was slightly lower than that of the DBTTP2 device, the maximum quantum efficiency of the DBTTP1 device was 18.7% at 150 cd m^{-2} . There are several factors affecting the quantum efficiency of the DBTTP1 and DBTTP2 devices, but hole and electron balance in the emitting layer can be regarded as the reason for the origin of the different quantum efficiency, because other factors such as energy transfer and charge confinement can be ignored due to the high triplet energy and similar energy levels of DBTTP1 and DBTTP2. Additionally, the higher PL quantum yield of the DBTTP2:4CzIPN film (100%) than that of the DBTTP1:4CzIPN film (62%) also increased the quantum efficiency of the DBTTP2 device. Doping concentration dependence of the quantum efficiency is presented in the ESI;† the quantum efficiency was optimized at 3%, which agreed with the PL intensity of the 4CzIPN doped film in the ESI.†

Lifetime test results measured at 1000 cd m^{-2} are presented in Fig. 7. The lifetime of the DBTTP1 device was longer than that of the DBTTP2 device at the same initial luminance of 1000 cd m^{-2} . The lifetime up to 80% of initial luminance was longer than 250 h for the DBTTP1 device, whereas it was shorter than 100 h for the DBTTP2 device. The longer lifetime of the DBTTP1 device than that of the DBTTP2 device can be analyzed from the viewpoint of the molecular structure of DBTTP1 and DBTTP2. The main difference in the molecular structure between DBTTP1 and DBTTP2 is the triphenylene and terphenyl moieties attached to the dibenzothiophene core. The triphenylene moiety has three aromatic units in the same plane and the dihedral angle between three aromatic units is almost 0° . However, the dihedral angle between the aromatic units of terphenyl is 38° and 39° as shown in Fig. 8. The large dihedral angle of the terphenyl moiety weakens the conjugation between aromatic units and leads to the accompanying weak chemical bond. Therefore, DBTTP2 with the terphenyl moiety is worse than DBTTP1 with the triphenylene moiety from the molecular structure point of view. From this result, it can be concluded that the triphenylene modified DBTTP1 can be effective as the host material of the 4CzIPN TADF dopant to secure stable lifetime. The lifetime of the highly doped DBTTP1 and DBTTP2 devices with 30% 4CzIPN doping concentration was also measured (ESI†), but it was reduced at high doping concentration due to the concentration quenching effect.

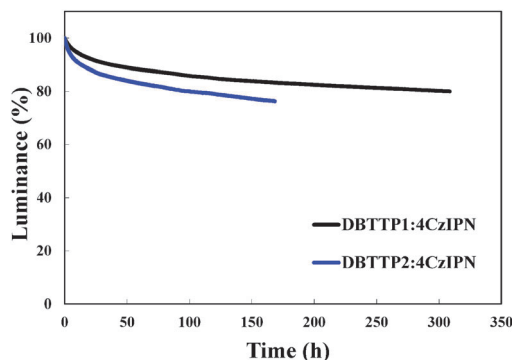


Fig. 7 Lifetime curves of DBTTP1:4CzIPN and DBTTP2:4CzIPN devices.

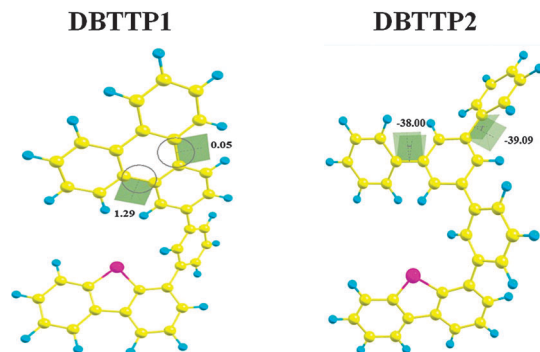


Fig. 8 Geometrical structures of DBTTP1 and DBTTP2.

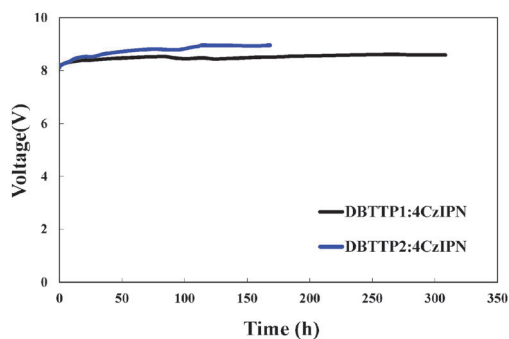


Fig. 9 Voltage change curves of the DBTTP1 and DBTTP2 devices during lifetime measurement.

Voltage change of the device according to the measurement time of the lifetime is shown in Fig. 9. Voltage rise during lifetime measurement was large for the DBTTP2 device, whereas it was relatively small for the DBTTP1 device. This result is associated with the lifetime of the device because luminance decrease according to the driving time is accompanied by an increase in the resistance of the device.

Conclusions

In summary, the effect of the molecular structure of the host materials derived from dibenzothiophene and aromatic moieties was studied, and it was revealed that the triphenylene moiety is more suitable as the aromatic moiety than the terphenyl moiety. The lifetime of the green TADF device was more than doubled when triphenylene based DBTTP1 was used instead of terphenyl based DBTTP2. Therefore, a molecule having the triphenylene

moiety can be effectively used as the host material to achieve a long lifetime for the green TADF device.

Acknowledgements

This work was supported by development of red and blue OLEDs with external quantum efficiency over 20% using delayed fluorescent materials funded by MOTIE.

References

- 1 B. Dias, N. Bourdakos, V. Jankus, C. Moss, T. Kamtekar, V. Bhalla, J. Santos, R. Bryce and P. Monkman, *Adv. Mater.*, 2013, **25**, 3707.
- 2 J. Lee, K. Shizu, H. Tanaka, H. Nomura, T. Yasuda and C. Adachi, *J. Mater. Chem. C*, 2013, **1**, 4599.
- 3 S. Wu, M. Aonuma, Q. Zhang, S. Huang, T. Nakagawa, K. Kuwabara and C. Adachi, *J. Mater. Chem. C*, 2014, **2**, 421.
- 4 J. W. Sun, J. H. Lee, C. K. Moon, K. H. Kim, H. S. Shin and J. J. Kim, *Adv. Mater.*, 2014, **26**, 5684.
- 5 Q. Zhang, B. Li, S. Huang, H. Nomura, H. Tanaka and C. Adachi, *Nat. Photonics*, 2014, **8**, 326.
- 6 Q. Zhang, D. Tsang, H. Kuwabara, Y. Hatae, B. Li, T. Takahashi, S. Y. Lee, T. Yasuda and C. Adachi, *Adv. Mater.*, 2015, **27**, 2096.
- 7 M. Kim, S. K. Jeon, S.-H. Hwang and J. Y. Lee, *Adv. Mater.*, 2015, **27**, 2515.
- 8 H. Uoyama, K. Goushi, K. Shizu, H. Nomura and C. Adachi, *Nature*, 2012, **492**, 234.
- 9 Y. J. Cho, K. S. Yook and J. Y. Lee, *Adv. Mater.*, 2014, **26**, 4050.
- 10 B. S. Kim and J. Y. Lee, *Adv. Funct. Mater.*, 2014, **24**, 3970.
- 11 M. P. Gaj, C. F.-H. Canek, Y. Zhang, S. R. Marder and B. Kippelen, *Org. Electron.*, 2015, **16**, 109.
- 12 T. Furukawa, H. Nakanotani, M. Inoue and C. Adachi, *Sci. Rep.*, 2015, **5**, 8429.
- 13 H. Nakanotani, K. Masui, J. Nishide, T. Shibata and C. Adachi, *Sci. Rep.*, 2013, **3**, 2127.
- 14 N.-J. Lee, J. H. Jeon, I. In, J.-H. Lee and M. C. Suh, *Dyes Pigm.*, 2014, **101**, 221.
- 15 B. Kim, Y. Park, J. Lee, D. Yokoyama, J.-H. Lee, J. Kido and J. Park, *J. Mater. Chem. C*, 2013, **1**, 432.
- 16 S.-C. Dong, L. Zhang, J. Liang, L.-S. Cui, Q. Li, Z.-Q. Jiang and L.-S. Liao, *J. Phys. Chem. C*, 2014, **118**, 2375.